Cosmological cooling of gas within dark matter halos

Aleix Albert Clotet, aalbercl51.alumnes@ub.edu
Facultat de Física, Universitat de Barcelona, Diagonal 645, 08028 Barcelona, Spain.

Advisor: Alberto Manrique Oliva, a.manrique@ub.edu

Abstract: This project explores the physics of radiative cooling in a cosmological context, focusing on the connection between cooling efficiency and halo mass. We begin by reviewing the main cooling mechanisms and their impact in the cooling function $\Lambda(Z,T)$. Then, we derive the analytical expressions for the cooling time t_{cool}, highlighting its dependence on gas density and radius. Finally, we implement a numerical code in Fortran to estimate the cooling radius for halos in the range $10^{8.6} - 10^{15}$ $M_\odot$ masses. Additionally, we compute the cooling time as a function of radius for a fixed halo mass. These results allow us to identify the regions where gas can effectively cool and potentially form stars.
Keywords: Gas cooling, DM halos, galaxy formation, cooling time, computation, baryonic infall.
SDGs: Quality education (num. 4).

I. Introduction

The formation of galaxies is a complex, multi-scale process involving both dark matter (DM) and baryonic gas. One of the key mechanisms that regulates galaxy formation is the radiative cooling of gas within DM halos. As gas falls into the gravitational potential wells created by halos, it heats up and must cool in order to collapse and form stars.

In the ΛCDM cosmological framework, galaxies form within DM halos that grow hierarchically through mergers and accretion. While DM drives the gravitational assembly of large-scale structure, it is the baryonic gas that radiates energy, cools, and forms stars—making galaxies observable.

Gas accreted into DM halos is initially shock-heated to the virial temperature (see eq. [7] for its definition), reaching values of $10^5 - 10^7$ K depending on the halo mass. Before significant star formation can occur, this hot, diffuse gas must cool and condense [1], a process that marks the transition from a primordial halo atmosphere to the early stages of galaxy formation.

In this work, we begin by outlining the theoretical background of gas cooling in DM halos. Section II.A introduces the key physical cooling processes, the formulation of the cooling time is shown in II.B, while II.C connects this framework to the simplified modelling adopted. Section III presents numerical results including the dependence of the cooling radius on halo mass in III.A and the radial profile of cooling time for fixed halo mass in III.B. Conclusions are presented in section IV.

II. Cooling Physics in Cosmological Halos

A. Radiative Cooling Mechanisms

The gas trapped into DM halos is in hydrostatic equilibrium at a quite high temperature. In these conditions, the ability of baryonic gas to cool radiatively within DM halos is a fundamental process governing galaxy formation. Further collapse requires the gas to lose internal energy. Radiative cooling is thus the key mechanism that regulates the conversion of baryons into stars [2].

The interplay between gravity, cooling, and feedback processes shapes the morphology, stellar mass, and evolution of galaxies. According to [3] if cooling is too efficient, simulations and models predict that halos would convert a large fraction of their gas into stars, overproducing stellar masses compared to observations. On the other hand, if cooling is too inefficient, galaxy formation is suppressed entirely.

Radiative cooling occurs through several physical mechanisms, each dominant in different temperature and density regimes. The net energy loss per unit volume due to these mechanisms is encoded in the cooling function $\Lambda(Z,T)$, which depends primarily on the gas temperature and metallicity [4].

The main cooling mechanisms explained in [1] include:

- **Atomic line cooling**, effective for $T \gtrsim 10^4$K, arises from collisional excitation and ionization of atoms and ions, followed by photon emission during de-excitation or recombination. It is especially efficient in metal-enriched gas and dominates in halos where virial temperatures are moderate.
- **Bremsstrahlung cooling** (free-free emission), becomes dominant at $T \gtrsim 10^7$K, where gas is fully ionized and electrons decelerate in the electric field of ions, emitting photons. It results in a smoother and less efficient energy loss, causing $\Lambda(Z,T)$ to decline at high temperatures. This explains why massive halos with high T_{vir} cool inefficiently despite their high densities.

- **Compton cooling**, relevant at high redshift $z \gtrsim 6$, involves energy transfer from free electrons to Cosmic Microwave Background (CMB) photons via inverse Compton scattering. This mechanism scales linearly with electron density and becomes negligible at low redshift.
- **Molecular hydrogen cooling**, crucial at low temperatures $T \lesssim 10^4$K, occurs in metal-poor environments where atomic cooling is ineffective. Cooling is provided by rotational and vibrational transitions in H_2 molecules, enabling the first episodes of star formation in minihalos in the early universe.

Together, these mechanisms define the shape of the cooling function $\Lambda(Z,T)$, which typically shows a peak near $10^4 - 10^5$K due to efficient line emission and decreases at both, lower (due to lack of atomic transitions) and higher (due to bremsstrahlung), temperatures.

In cosmological models, $\Lambda(Z,T)$ is usually computed assuming collisional ionization equilibrium (CIE), and tabulated for different metallicities. It definitely is a critical ingredient for modeling thermal evolution and star formation in halos of different masses.

B. Cooling time and the role of gas density

The cooling time of a gas represents the timescale over which it loses its internal energy via radiative processes. It is defined as the ratio between the thermal energy content of the gas and its radiative loss rate per unit volume. Assuming a fully ionized plasma with primordial composition, the internal energy per unit volume is given by:

$$u = \frac{3}{2} n k_B T, \tag{1}$$

where n is the total number density of particles, k_B the Boltzmann constant, and T the temperature. The cooling rate per unit volume can be written as:

$$\dot{u} = n_e n_i \Lambda(Z,T), \tag{2}$$

where n_e is the electron's density, n_i the ions density and $\Lambda(Z,T)$ the cooling function. For a fully ionized gas $n_e \approx n_i \approx n/2$ and hence $\dot{u} \sim n^2 \Lambda(Z,T)$. If we integrate both sides of (2) and substitute in equation (1) we obtain that the cooling time becomes:

$$t_{cool} = \frac{3 k_B T}{2 n \Lambda(Z,T)}. \tag{3}$$

In galaxy formation models, it's common to express the cooling time in terms of mass density ρ_g instead of particle number density. Using the relation $n = \rho_g/(\mu m_p)$, where μ is the mean molecular weight and m_p the proton mass [3], the cooling time can also be expressed as:

$$t_{cool} = \frac{3 k_B T \mu m_p}{2 \rho_g \Lambda(Z,T)}. \tag{4}$$

This expression directly shows that the cooling time is inversely proportional to the gas density. Higher densities lead to more efficient cooling, while lower densities significantly delay the process.

In our calculation, we adopt a power-law gas density profile that scales as r^{-2}. When this form is inserted into the equation of hydrostatic equilibrium and combined with the ideal gas law [1], it yields an isothermal solution with a temperature equal to the virial temperature of the halo:

$$\rho_g = \frac{k_B T_{vir}}{2\pi G m_p r^2}, \tag{5}$$

where G is the gravitational constant and T_{vir} the virial temperature previously mentioned. This profile reflects the expected drop in density with the radius of the halo. When substituted into equation (4), it leads to this radial dependence of the cooling time:

$$t_{cool} \propto r^2. \tag{6}$$

It is important to note that the classical formulation of this model, based on the assumption that each shell of gas cools independently after one local cooling time, was first implemented in the semi-analytical model [5]. While this approach captures the essential physics, it neglects several complexities such as the back-reaction of cooling or non-isobaric effects. More recent frameworks, such as the model [6], have introduced refinements to account for a more gradual transition between hot and cold phases and improve the fidelity of the cooling flow predictions.

C. Cooling time as a diagnostic

While the physics of gas cooling in halos can be modeled with detailed hydrodynamic simulations and semi-analytic approaches, these models often involve complex, time-dependent behavior, evolving metallicities and energy input from feedback mechanisms [2].

In contrast, our approach adopts a simplified, yet physically meaningful, prescription. The model assumes a spherically symmetric, isothermal gas distribution in hydrostatic equilibrium within an isolated DM halo. By neglecting any external heating or dynamical effects, the system is reduced to a static configuration where cooling depends only on halo mass, radius, and the cooling function.

Using this prescription, we compute two main diagnostics. First, we determine the cooling radius over a given timescale, typically taken to be the Hubble time or fractions of it. Second, we evaluate the cooling time profile for fixed halo masses, mapping how the efficiency of cooling varies across radial shells.

Despite its idealized nature, this framework retains the essential physical dependencies and provides valuable insight into the conditions under which galaxy formation is expected to be efficient. Moreover, it serves as a conceptual and computational stepping stone between fully analytical models and more sophisticated numerical simulations.

III. Numerical implementation and results

The previous section presented the theoretical basis for understanding the radiative cooling of gas within DM halos. In this section, we implement that framework numerically to investigate two key quantities:

- The cooling radius r_{cool}, defined as the radius within which gas has had time to cool over diferent ages.
- The cooling time $t_{cool}(r)$, calculated for fixed halo masses at different radial positions.

These two complementary approaches offer insights into the thermodynamic behaviour of baryonic gas in halos under simplified conditions, namely, in the absence of any feedback mechanisms such as supernovae or AGN heating.

The numerical computations are performed using a Fortran code specifically developed for this project. The program takes as input a tabulated cooling function $\Lambda(Z,T)$, taken from [4], which does not include the molecular hydrogen cooling mechanism described in Section II.A.

Each DM halo is modelled as an isolated, spherically symmetric system, with the baryonic gas initially in hydrostatic equilibrium at the virial temperature (isothermal profile). The code employs Brent's method to solve the non-linear equation defining the cooling radius, and uses spline interpolation routines to ensure a smooth and reliable evaluation across the temperature range.

A. Cooling radius as a function of halo mass

In the first numerical experiment, we study how the cooling radius r_{cool} varies with halo mass. The goal is to determine which halos can cool a significant fraction of their baryonic gas within a given cosmological time and, consequently, are more likely to support efficient star formation.
For each halo mass between $10^{8.6}\mathrm{M}_\odot$ and $10^{15}\mathrm{M}_\odot$, the virial radius R_{vir}, the radius within which dark matter is virialized, and T_{vir}, which characterizes the gravitational potential energy of the halo, are computed using:

$$R_{vir} = \left(\frac{3M_{halo}}{4\pi 200\rho_{crit}}\right)^{1/3}; T_{vir} = \frac{2}{3}\frac{GM_{halo}\mu m_p}{R_{vir}k_B}, \quad (7)$$

where ρ_{crit} is the critical density of the Universe and $\mu = 0.6$ is the mean molecular weight. For the present-day Universe (t_0), we adopt $\rho_{crit} = 9.2 \cdot 10^{-27}\mathrm{Kg/m}^3$. For earlier epochs, the values are adjusted according to the evolving background cosmology. We assume a flat ΛCDM model with present values $\Omega_m = 0.3$ and $\Omega_\Lambda = 0.7$, ensuring a consistent computation.

The gas is taken to be initially at the virial temperature and distributed in hydrostatic equilibrium, following the assumptions described in Section II. Based on this setup, the local cooling time at each radius is:

$$t_{cool}(r) = \frac{3}{2}\frac{k_B T_{vir}\mu m_p}{\rho_g(r)\Lambda(Z,T_{vir})}, \quad (8)$$

where $\rho_g(r)$ refers to the radial gas density profile previously shown in equation (5), and $\Lambda(Z,T_{vir})$ is the cooling function, interpolated from a dataset. This function plays a central role in this process and will define the shape of our figure. The cooling radius is determined by:

$$t_{cool}(r_{cool}) = t. \quad (9)$$

The cooling radius is calculated for three cosmic times: t_0, $\frac{3}{7}t_0$ and $\frac{4}{17}t_0$, corresponding to redshifts $z = 0$, 1 and 2, respectively. Since the critical density of the Universe evolves with redshift, different values are used in each case.

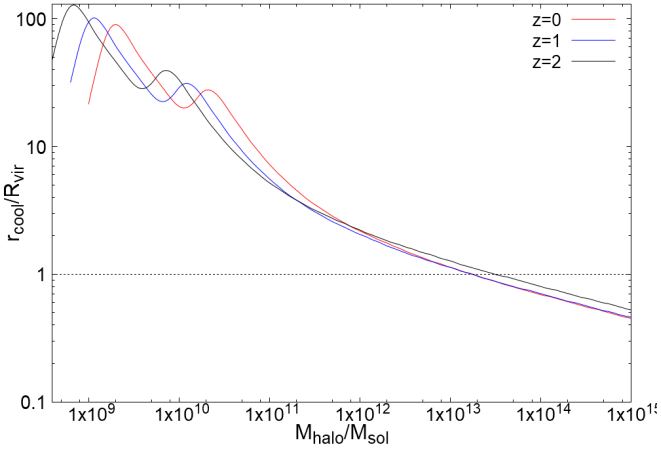

FIG. 1: Cooling radius r_{cool}/R_{vir} as a function of halo mass for three different cooling times: t_0 (red), $\frac{3}{7}t_0$ (blue), and $\frac{4}{17}t_0$ (black). Both axis are on a logarithmic scale, and there is a dashed black line in $r_{cool} = R_{vir}$.

As expected, the cooling radius becomes progressively smaller as the assumed cooling time is reduced. This is a direct consequence of the physical definition of the cooling radius: only regions where the gas density is high enough can radiate energy fast enough to cool. This effect is particularly noticeable in intermediate-mass halos, where the gas profile steepens, and the cooling efficiency drops off quickly with radius.

Examining the graph, all three curves follow a similar overall shape but exhibit noticeable shifts in both position and amplitude. As the redshift increases (from red to blue to black), the peaks move toward lower halo masses and become more pronounced. This behavior reflects the combined impact of shorter cosmic timescales and higher critical densities at earlier epochs.

Although less time is available for gas to cool, the higher background density enhances the cooling rate in the central regions, which explains the higher peak values. Consequently, halos of lower mass reach the cooling threshold more efficiently at higher redshifts, but this effect is limited to their innermost regions. The physical origin of these features becomes clearer when analyzing the three main halo mass regimes (for t_0):

- At low masses ($M_{halo} \lesssim 10^9 M_\odot$), virial temperatures are relatively low ($T_{vir} \sim 10^4 - 10^5$K), close to the lower end of the cooling function's efficiency range. Although atomic cooling begins to operate, it is not yet optimal. Moreover, cooling becomes inefficient below 10^4K, and molecular cooling is not included in our model. As a result, the cooling radius drops sharply for these small halos, especially at high redshift, where the time available for cooling is even more limited.

- At intermmediate masses ($10^9 M_\odot \lesssim M_{halo} \lesssim 10^{11} M_\odot$), halos in this range exhibit virial temperatures ($10^4 - 10^5$K) that match the peak of the cooling function, where atomic line emission is most effective. This leads to extended cooling radius, particularly at lower redshift, where there is more time for gas to radiate its energy. Interestingly, the denser environment can still support efficient cooling in less massive systems for larger redshifts.

- At high masses ($M_{halo} \gtrsim 10^{12} M_\odot$), virial temperatures exceed 10^6K, entering the bremsstrahlung-dominated regime where the cooling function decreases with increasing temperature. Despite the higher densities, the cooling efficiency drops significantly, and the cooling radius becomes confined to the very central regions. The shift of the curves also shows that this suppression becomes more pronounced at higher redshift.

In halos where the gas temperature matches the peak of $\Lambda(Z,T)$, cooling is extremely efficient. Outside this range, particularly for very hot halos, radiative losses are suppressed, resulting in longer cooling times and smaller cooling radius.

These results confirm theoretical predictions from models such as [5], who proposed that galaxy formation is primarily efficient in halos where the cooling time is shorter than the dynamical time, typically for halo masses around $10^9 - 10^{10} M_\odot$.

This interpretation is reinforced by the behaviour of $\Lambda(Z,T)$, plotted bellow:

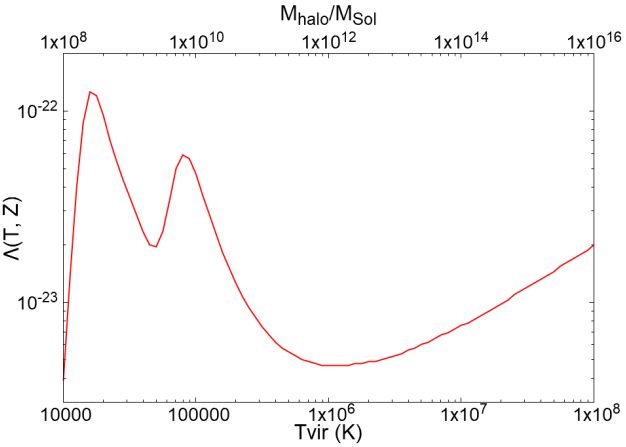

FIG. 2: Cooling function $\Lambda(Z,T)$ as a function of temperature T_{vir}(bottom axis). The top axis shows the corresponding halo mass M_{halo} derived from the T_{vir}. Both x-axes and y-axis are on a logarithmic scale.

Moreover, this behaviour explains observed trends in the galaxy luminosity function, where a sharp cutoff is seen at the bright end, a signature of suppressed cooling.

B. Cooling time as a function of radius

This section explores the radial variation of the cooling time within DM halos of different masses. This approach offers insight into the internal structure of halos and helps identify which regions are thermodynamically capable of losing energy and condensing into stars. The results are shown for three halo masses: 10^{12}, 10^{13} and 10^{14} $M_\odot$:

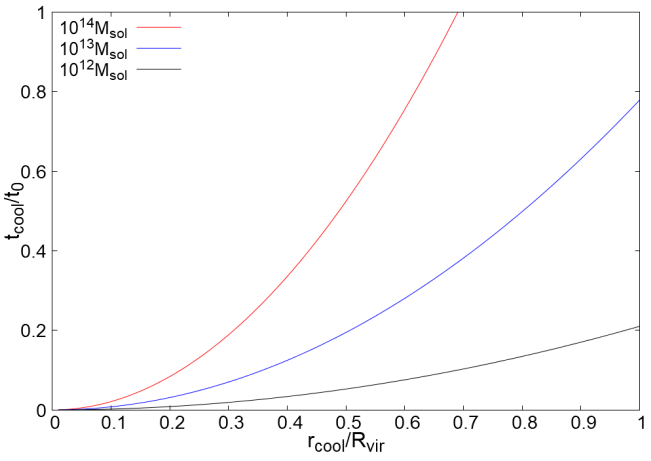

FIG. 3: Cooling time t_{cool}/t_0 as a function of cooling radius r_{cool}/R_{vir} for halos of mass $10^{12} M_\odot$ (black), $10^{13} M_\odot$ (blue), and $10^{14} M_\odot$ (red).

The cooling time increases monotonically with radius for all three halo masses. Since the virial temperature is fixed in each case, the cooling function remains constant across the profile, and the rise in $t_{cool}(r)$ is entirely driven by the declining gas density. The y-axis has been limited as a reference: the point where each curve intersects this mark the maximum radius within which gas has time to cool over a Hubble time.

In the $10^{12}M_\odot$ case, the cooling time remains quite below the age of the Universe across most of the halo, up to nearly the virial radius. This indicates that the majority of the gas has had sufficient time to cool and potentially participate in galaxy formation. The corresponding virial temperature lies near the peak of the cooling function, where is most efficient. This combination of favourable thermodynamic conditions results in a halo with nearly optimal cooling efficiency.

In the $10^{13}M_\odot$ halo, the cooling time remains below the Hubble time up to nearly the virial radius, though less comfortably than in the $10^{12}M_\odot$ case. This suggests that gas can still cool efficiently on large scales, although with reduced margin.

In contrast, the $10^{14}M_\odot$ halo shows a much sharper rise in cooling time, exceeding the Hubble limit well after reaching half of R_{vir}. At these high temperatures, cooling enters the bremsstrahlung-dominated regime, where $\Lambda(Z,T)$ declines with temperature, and most of the halo remains hot. Only the central region retains realistic chances for radiative cooling and collapse.

These results confirm that cooling is not uniformly efficient across a halo, and that this efficiency decreases with increasing halo mass. From a physical standpoint, the balance between gas density and temperature becomes increasingly unfavourable in massive systems, where only a small central region is dense and cool enough to radiate efficiently.

As a consequence, galaxy formation in these environments is highly concentrated and inefficient unless other mechanisms (such as mergers or AGN-driven outflows) intervene.

IV. Conclusions

In this work, we have explored the radiative cooling of baryonic gas within DM halos using an analytical and numerical framework rooted in hydrostatic equilibrium and idealized thermodynamic conditions. By deriving explicit expressions for the cooling time and its dependence on gas density, we have demonstrated how cooling efficiency varies.

Our numerical results, based on a Fortran implementation, show that cooling is most efficient in halos with virial temperatures near $10^4 - 10^5$K, corresponding to halo masses around $10^9 - 10^{10}M_\odot$. These masses align with the peak of the atomic cooling function, suggesting a strong correlation between thermodynamic conditions and the expected efficiency of galaxy formation.

At higher masses, bremsstrahlung dominates and cooling becomes suppressed despite higher densities, while at lower masses, the absence of molecular cooling leads to long cooling times, especially at high redshift.

The radial dependence of the cooling time further confirms that only the inner fraction of massive halos, typically within $\sim 0.7R_{vir}$, has enough time to cool within a Hubble time. This supports the idea that star formation in such systems is confined to central regions, though not strictly limited to the very core. These findings are consistent with predictions from semi-analytic models like [5] and provide a physically grounded, yet computationally accessible, framework to interpret cosmological structure formation.

Although simplified, our model captures the essential physics and offers a base for future extensions incorporating dynamical infall, metal enrichment, and feedback processes.

Acknowledgments

I must thank my advisor Dr. Alberto Manrique for his advice and his guidance during this project, without which this would not have been possible. I would also like to thank my family, friends and girlfriend for their unconditional support.

[1] M. Viola, P. Monaco, S. Borgani, G. Murante and L. Tornatore, *How does gas cool in DM halos?*, (Monthly Notices of the Royal Astronomical Society, 2007).
[2] J. Benson, *Galaxy formation theory*, (Physics Reports, vol. 495, p. 33–39, 2010).
[3] P. Laursen, *Galaxy Formation from a Timescale Perspective*, (Multiplicity of Timescales in Complex Systems, 2023).
[4] R. Sutherland and M. Dopita, *Cooling functions for low-density astrophysical plasmas*, (The Astrophysical Journal Supplement Series, vol. 88, p. 253–327, 1993).
[5] S. White and C. Frenk, *Galaxy Formation Through Hierarchical Clustering*, (The Astrophysical Journal, vol. 379, p. 52-79, 1991).
[6] P. Monaco, F. Fontanot and G. Taffoni, *The MORGANA model for the rise of galaxies and active nuclei*, (Monthly Notices of the Royal Astronomical Society, vol. 375, p. 1189–1219, 2007).

Refredament cosmològic del gas dins dels halos de matèria fosca

Aleix Albert Clotet, aalbercl51.alumnes@ub.edu
Facultat de Física, Universitat de Barcelona, Diagonal 645, 08028 Barcelona, Spain.

Advisor: Alberto Manrique Oliva, a.manrique@ub.edu

Resum: Aquest projecte explora la física del refredament radiatiu en un context cosmològic, centrant-se en la connexió entre l'eficiència de refredament i la massa de l'halo. Comencem revisant els principals mecanismes de refredament i el seu impacte en la funció de refredament $\Lambda(Z, T)$. A continuació, derivem les expressions analítiques per al temps de refredament t_{cool}, destacant la seva dependència de la densitat del gas i el radi sota la suposició d'equilibri hidrostàtic. Finalment, implementem un codi numèric en Fortran per estimar el radi de refredament per a halos en el rang de masses $10^{8.6} - 10^{15}$ $M_\odot$. A més, calculem el temps de refredament com a funció del radi per a una massa d'halo fixa. Aquests resultats ens permeten identificar les regions on el gas es pot refredar eficaçment i potencialment formar estrelles.
Paraules clau: Refredament del gas, halos de matèria fosca, formació de galàxies, temps de refredament, computació, caiguda bariònica.
ODSs: Educació de qualitat (núm. 4)